

Distribution and Variation of Pressure and Temperature in Wood Cross Section during Radio-Frequency Vacuum (RF/V) Drying

HongHai Liu,^a Lin Yang,^a Yingchun Cai,^b Kazuo Hayashi,^c and KaiFu Li^{a,*}

The pressure and temperature at the same location in the middle cross section of Sugi wood were measured simultaneously during radio-frequency/vacuum (RF/V) drying. The distribution and variation of pressure and temperature in the wood cross section were investigated in different drying stages. The pressure behavior during the drying process was due to the pressure reduction rate and water vapor generation rate in wood. The temperature was higher in the center and was low from the center to surface layer. Pressure and temperature did not present symmetrical distributions along the vertical direction in the cross section. The pressure was irregular during the timber heating stage and became higher in the central zones than in the intermediate and surface layer zones during the drying process. Pressure curves exhibited three stages (irregular, rapid decreasing, and slow decreasing), in combination with an initial heating stage and a constant temperature stage. Above the fiber saturation point (FSP), the pressure (P) was greater than or equal to the saturated vapor pressure (P_s), corresponding to the temperature at the same location; below the FSP the pressure was maintained by superheated vapor and was smaller than P_s .

Keywords: Radio frequency/vacuum drying; Temperature and pressure; Distribution in wood cross section; Superheated vapor

Contact information: a: College of Forestry, South China Agricultural University, 483 Wushan Road, Tianhe District, GuangZhou 510642, China; b: Key Laboratory of Bio-based Material Science and Technology, Northeast Forestry University, Harbin 150040, China; c: Department of Forest Resources, Faculty of Agriculture, Ehime University, 3-5-7 Tarumi, Matsuyama 790-8566, Japan;

* Corresponding author: kfli@scau.edu.cn

INTRODUCTION

Wood drying is an essential step in the manufacture of wooden products. However, conventional kiln drying is a time-consuming and energy-intensive process. Compared with conventional kiln drying, radio-frequency vacuum (RF/V) drying has many advantages, such as shorter drying time, suitability for large dimensions of timber, lower risk of discoloration, and better energy efficiency (Ressel 1994; Welling 1994). As a special drying method, RF/V drying has been applied in industry for the last few decades and is likely to be more widely used. A reduction in drying time and/or an improvement in the quality of the dried timber offers potential economic benefits. Therefore, for RF/V drying, improvements in the wood drying process will be facilitated by a greater understanding of the drying process, especially moisture distribution and transfer in wood, because it is directly related to internal stress development and drying defects.

Studies have been carried out on the mechanisms of moisture transfer under vacuum drying (Anastasios *et al.* 2001; Cai *et al.* 2001; Zhang *et al.* 1997). Most work supports the assumption that the driving force is caused by the pressure gradient. During RF/V drying, a steep pressure gradient along with a temperature gradient is developed from the center towards the surface of timber. The pressure gradient helps to quickly drive out wood moisture in both liquid and vapor form. As the pressure approaches and exceeds the boiling point of water, rapid vapor generation inside wood may produce a significant total pressure gradient in addition to partial vapor pressure gradients (Waananen and Pkos 1989) to move water vapor from a high pressure region to a low pressure region under total pressure difference. Total pressure differences inside a porous medium have recently been used to identify the importance of a bulk flow mass transfer mechanism at temperatures above the boiling point of water for vacuum drying. Noack (1965) found that moisture migrates during vacuum drying in a gas state (steam) when wood dries below the fiber saturation point (FSP).

Therefore, pressure is an important factor in moisture transfer in wood during special drying, such as high-temperature drying and RF/V drying. Some studies (Avramidis *et al.* 1994; Perre and Mosnier 1995; Sasaki *et al.* 1987; Taniguchi and Nishio 1993a, b) on RF/V drying have been carried out for the measurement of temperature and pressure, although the pressure and temperature measured were not in the same location. Research (Cai *et al.* 2001; Cai and Hayashi 2001, 2002) predicted that above the FSP, the pressure in wood was equal to the saturated vapor pressure; the cited authors also estimated the pressure distribution according to the temperature detected during RF/V drying, although no experiments were carried out to verify its validity. It is known that there is a broad temperature distribution in RF/V drying (Anastasios *et al.* 2001; Resnik *et al.* 1997; Zhang *et al.* 1997); thus, simultaneous temperature and pressure measurement in the same location becomes very important to investigate the relationship of temperature, pressure, and moisture content (MC) in RF/V drying. Although Cai and Hayashi (2007) and Liu *et al.* (2010) measured temperature and pressure simultaneously at the same locations in wood during RF/V drying, real time MC monitoring was the objective. No investigations have been carried out to determine temperature and pressure distributions at cross sections and for the verification of the relationship between total pressure and saturated vapor pressure above FSP and/or below FSP. Therefore, in this study, the temperature and pressure at the same middle cross section location in Sugi timber was measured simultaneously to investigate the distribution of pressure and temperature and the relationship between total pressure and saturated vapor pressure as well as the relationship between pressure, temperature, and MC during RF/V drying.

EXPERIMENTAL

Materials

Sugi wood (*Cryptomeria japonica* D. Don, 55.8% initial MC, 0.32 g/cm³ basic density) box-heart square timber with dimensions of 500 cm (L) × 12 cm × 12 cm was divided into five end-matched parts, with the final sample size for pressure and temperature distribution tests 85 cm (L) × 12 cm × 12 cm (Fig. 1).

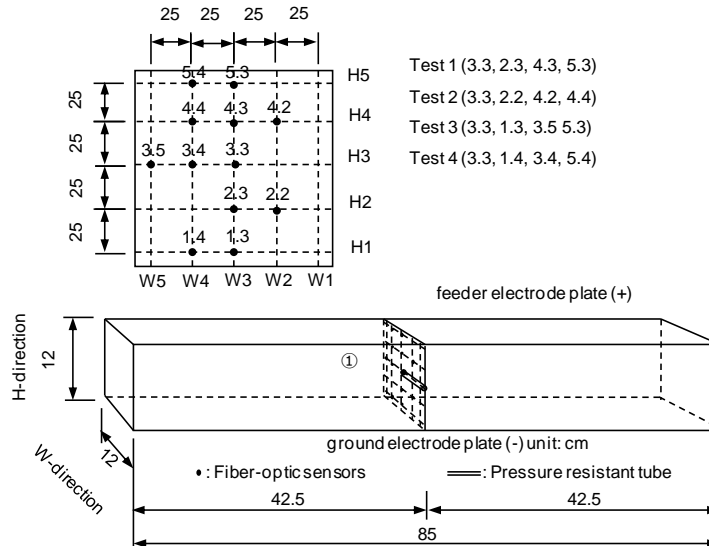


Fig. 1. Sample dimensions and locations in cross section for temperature and pressure measurement under RF/V drying. The measurement locations are expressed by two numbers; the first number shows the location in the H direction (thickness) and the second number shows the location in the W direction (width). H, thickness direction against electrode plate; W, width direction

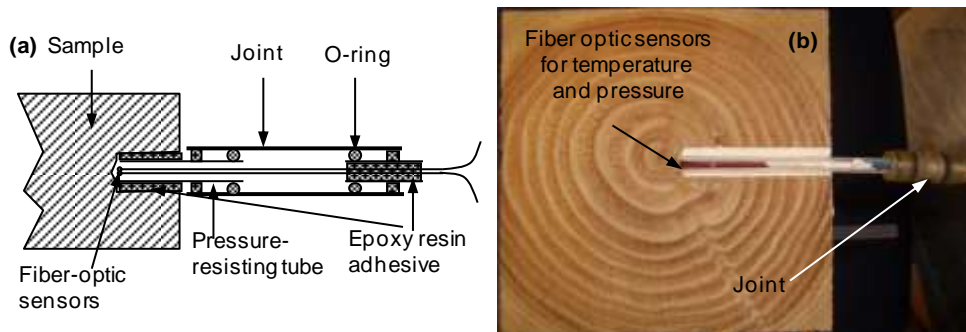


Fig. 2. Temperature and pressure measurement sensor complex unit under RF/V drying. (a) schematic and (b) actual photo

Methods

Temperature and pressure optical sensors were combined as a complex unit (Fig. 2). The wood sample was drilled at designated locations, and then the plastic pressure resisting tube was inserted in the drilled holes and glued with samples. The complex unit was connected with the plastic tube through the joint before and after drying. Temperature and pressure were measured at the same location simultaneously through a data logger and software once every 3 min during the drying process at four locations (Fig. 1).

Because one test can only obtain data from four locations, a total of four tests were carried out to investigate temperature and pressure distribution in this study. The test number and corresponding measurement location are shown in Fig. 1. In addition, another test was carried out to obtain MC during the drying process; in this test, the sample was removed from the chamber at specified time points for weight and MC measurement. In every test, temperature was controlled at the central location designated

as T3.3 (setting value is 60 °C), and the ambient pressure was controlled at 6.7 kPa; the radio-frequency (RF) loading and chamber evacuation were initiated simultaneously. The RF generator was set at a frequency of 27 MHz, with a rated output of 1 kW at an electrode RF voltage of 1 kV. The RF load was controlled by temperature and time, with the latter having priority. The term temperature control means that the RF load was stopped when T3.3 reached the setting temperature and was restarted when T3.3 was 2 °C lower than the setting temperature. The time control was set to 9 min, with an RF load and a 3-min unload of RF throughout the drying process.

RESULTS AND DISCUSSION

General Variation of Pressure, Temperature, and Moisture Content during Drying

The pressure and temperature at the locations investigated during drying and the average MC *versus* time are plotted in Fig. 3. It can be seen that the temperature curves generally exhibited two stages, the increasing stage and the constant stage (drying stage). Corresponding to these two stages, the pressure curves showed three stages that were an irregular decreasing stage corresponding to a temperature increasing stage, a steep decreasing stage, and a slow decreasing stage corresponding to a temperature constant stage. In addition, it can be seen that above the FSP, the drying rate was high; below the FSP, the drying rate decreased.

During the drying process, the highest temperatures were found in the central location, then in intermediate zone locations; the lowest temperatures were in outer zone locations near side surfaces. Although heat was generated within wood through oscillation of water dipoles and ions in the lumen and cell walls, temperature distribution in wood cross-section was not constant for the effects of latent heat of evaporation, heat conduction, thermal radiation, and permeability of wood. Pressure behavior was primarily affected by the rate of pressure reduction and vapor generation, as well as by the distance to the wood surface and the permeability of the wood.

The pressure in outer zones decreased quickly due to the short distance to the wood surface, while the pressure at the central location decreased slowly not only for the long distance to ambient pressure, but also because of the higher temperature, which generated higher vapor pressure above the FSP. Below the FSP, the pressure at all locations decreased slowly because the vapor generation rate decreased, resulting in small pressure differences and a decreased drying rate.

There have been some studies (Anastasios *et al.* 2001; Koumoutsakos *et al.* 2003) on the mass and heat transfer modeling for RF/V drying. A two-dimensional model has been found the yield more realistic and improved predictions in temperature profile based on the comparison with tests results. Compared with the temperature predictions results of the two-dimensional model, although with different drying schedule and controlling temperature, the temperature curves in this study presented similar trend both in MC above or below FSP, meanwhile the MC variation also behaved similar. Therefore, the study on temperature, pressure and MC distribution was also useful for drying mechanism analysis through modeling.

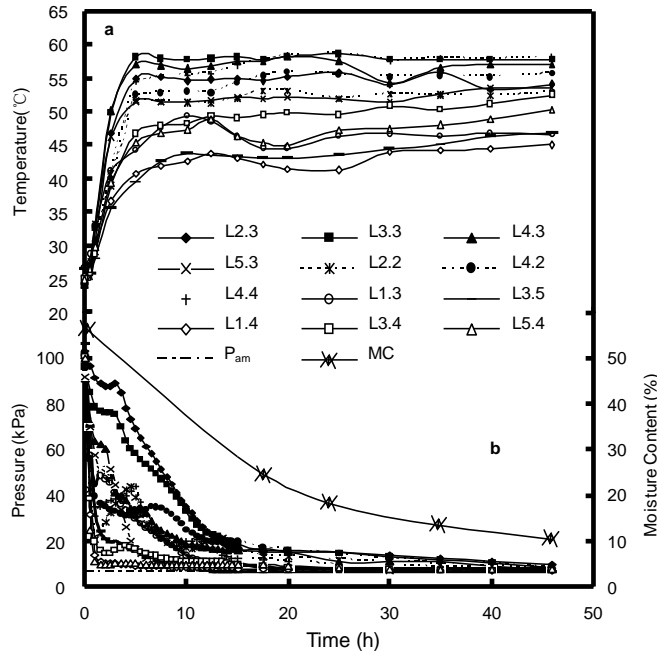


Fig. 3. Temperature and pressure curves of locations at a middle cross section during the drying process: (a) temperature and (b) pressure. P_{am} , ambient pressure; MC, average moisture content

Distribution and Variation of Pressure and Temperature in Wood Cross Section during Timber Heating Stage

The pressure and temperature variation curves corresponding to all locations are plotted in Fig. 4a, 4b, and 4c during the heating stage. Figure 4a shows the curves of the locations at central vertical (H direction) zones in the cross-section where locations are near the ground electrode plate to the center and then to the feeder electrode plate. Figure 4b shows the curves of the locations at intermediate zones around the center. Figure 4c shows the curves of the locations at the surface zones.

The temperature of all detected locations increased in the first 5 h during the timber heating stage. In Fig. 4a, the central location L3.3 (temperature controlling location) reached and retained the top temperature, followed by L4.3 (which behaved almost the same as L3.3), L2.3, L5.3, and L1.3. The temperature of location 1.3 and 5.3 near the electrode plate was lower due to release of latent heat of vaporization and heat lost by conduction to the metal electrode plate; the same phenomenon occurred at L1.4 and L5.4 (Fig. 3). Compared to the L4.3 temperature, L2.3 was lower, perhaps since it was closer to the ground electrode plate where more heat was transferred toward the ground electrode plate. Generally, along the H direction, temperature in minus direction (toward to ground electrode plate) was lower than the temperature at same opposite location in the plus direction (toward to feeder electrode plate).

During the heating stage, RF loading was combined with chamber evacuation; thus pressure in the wood was affected by the pressure reduction rate and the vapor evaporation rate. Pressure reduction was influenced by wood permeability and distance to the wood surface. Above the FSP, the vapor evaporation was influenced by temperature, with higher temperature causing higher saturated pressure. As seen in Fig. 4a, the pressure decreased quickly in the first hour and then increased somewhat, to finally decrease continuously. From the beginning, the pressure reduction rate was faster than

the vapor generation rate for the low initial temperature; after about one hour of drying, the vapor generation rate was greater than the pressure reduction rate for the increased temperature, finally resulting in the total pressure increasing at different rates in different locations. For L2.3 and L3.3, the pressure started decreasing once the temperature became constant, which means that the pressure reduction rate was higher than the vapor generation rate because vapor generation was constant for the constant temperature above FSP. This phenomenon at the other three locations began earlier as compared to these two locations. For L4.3 and L2.3 at the opposite side of the center, even at almost an identical temperature, the pressure behaved quite differently due to a fast pressure reduction rate at L4.3. In Fig. 4a, the locations with the fastest pressure decrease were L1.3 and L5.3, which were close to the surface, resulting in an easy reduction in pressure.

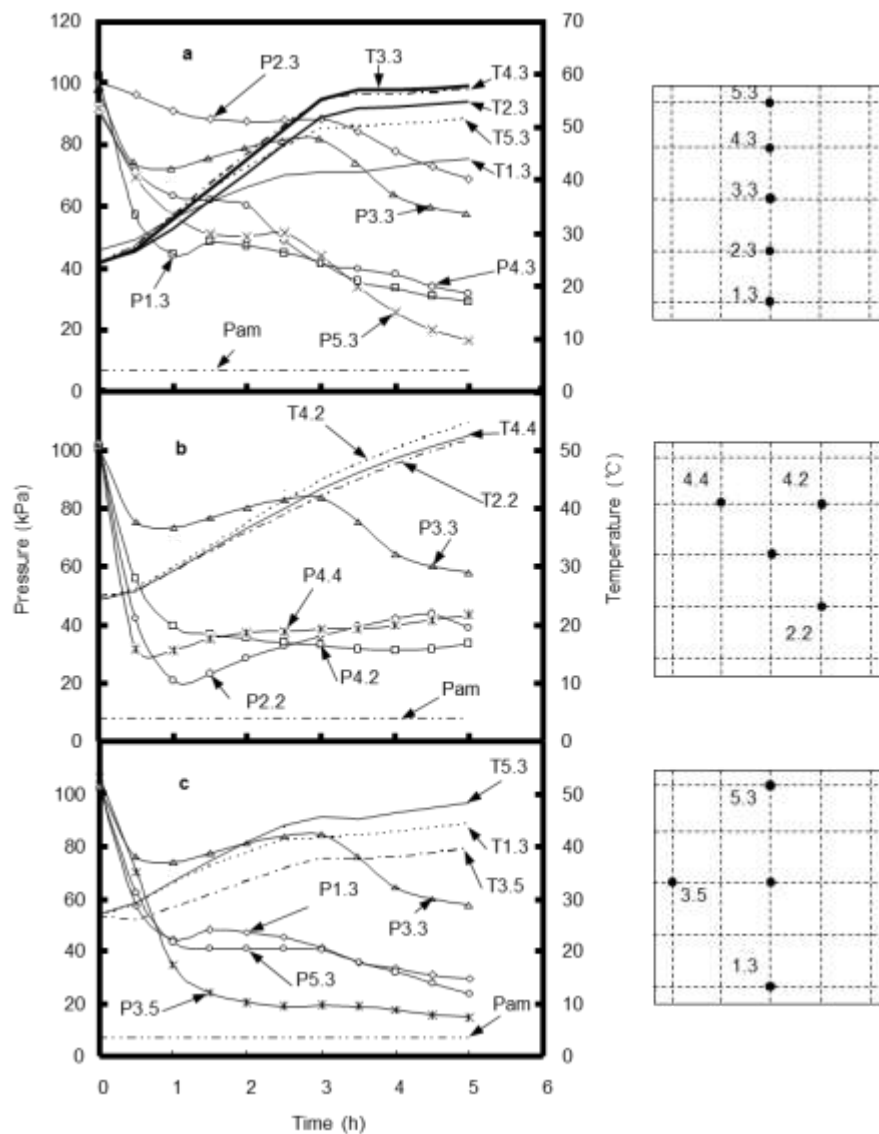


Fig. 4. Pressure and temperature variation during the temperature increasing stage: (a) in central vertical zones, (b) in intermediate layer zones, and (c) in surface layer zones

The slowest pressure decreasing location was not L3.3 but L2.3, where permeability was poor compared with central zone L3.3. The temperature and pressure of L4.4, L4.2, and L2.2 in the intermediate zone was similar (Fig. 4b). Temperature increased continuously, pressure decreased quickly to lowest point, and then either increased or decreased. Compared to the central location, temperature and pressure were lower in the intermediate zone. For the outer zone layer at L1.3, L5.3, and L3.5, the temperature was lower than in the intermediate zone; after decreasing, the pressure increased slightly or kept decreasing because the evaporated water vapor pressure was not sufficient to counteract the pressure reduction upon approach to the wood surface.

The pressure and temperature distributions after 2.5 h are plotted in Fig. 5a and Fig. 5b, respectively. We can see intuitively that the temperature was higher in the center, lower in the intermediate layer, and lowest at the surface; for pressure, due to the interaction of pressure reduction and vapor generation, the pressure distribution was irregular.

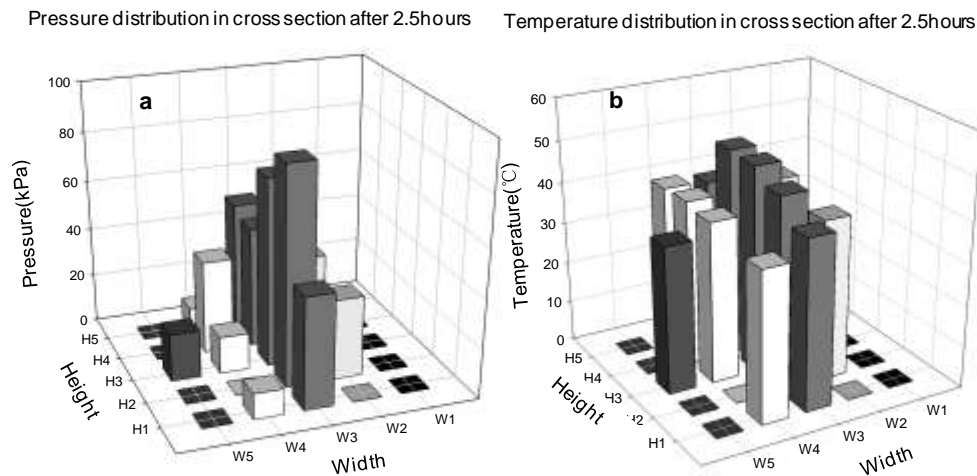


Fig. 5. Pressure and temperature distribution in a cross-section after 2.5 h: (a) pressure distribution and (b) temperature distribution

Distribution and Variation of Pressure and Temperature in Wood Cross-section during Timber Drying Stage

Figures 6a, b, and c illustrate the pressure and temperature variation curves of the locations during the drying stage. It can be seen from Fig. 6a, b, and c that after temperature reached the controlling temperature, the pressure showed a decreasing tendency, including a fast decrease above the FSP and a slow decrease below the FSP, while the temperature remained relatively constant with the tendency from a high value at the central zone to become a low value at the surface layer. Above the FSP, free water was easily evaporated and removed from wood, while below the FSP, bound water generation became difficult and evaporation became difficult, and it took more time for the bound water to be removed. At the central vertical zones after 15 h (Fig. 6a), pressure was high in the center and low in both surface zones with a big pressure difference. Pressure in L4.3 at a high temperature was lower than L2.3 with low temperature, which shows that pressure was affected not only by temperature but also by local permeability (pressure is easy to release for locations with good local permeability).

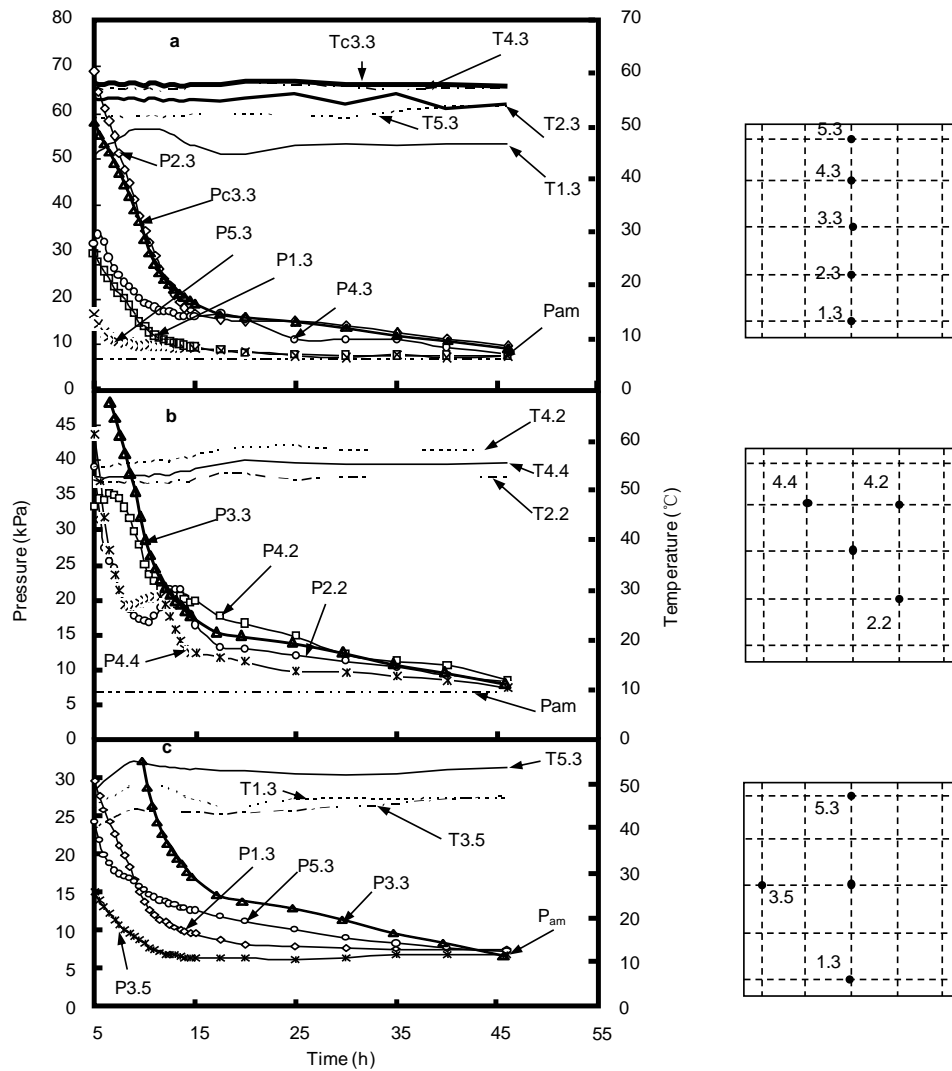


Fig. 6. Pressure and temperature distribution of various locations during drying stage: (a) central vertical zones, (b) in intermediate layer zones, and (c) in surface layer zones

This phenomenon can also be seen in Fig. 6b for L2.2 and L4.4. However, for the surface layer zones in Fig. 6c, which had almost the same permeability, the temperature increased with increasing pressure because the pressure was affected mainly by temperature. Furthermore, the pressure difference between the center and the intermediate zones was small, while it was bigger between the center and the surface zones.

Pressure and temperature distribution after 20 h and at the end of drying (after 46 h) are plotted in Figs. 7 and 8. There is a greater pressure gradient in the cross-section at 20 h than that at the drying end. The pressure gradient from the center zone to the surface layer zones became smaller as drying continues. The temperature gradient in cross-section at 20 h was not as big as the pressure gradient, and remained relatively constant as drying continued.

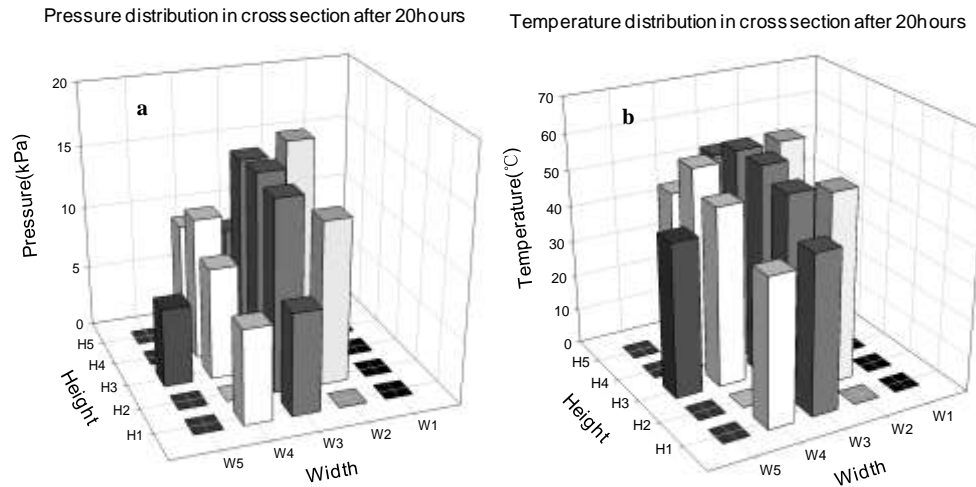


Fig. 7. Pressure and temperature distribution in cross-section after 20 h: (a) pressure distribution and (b) temperature distribution

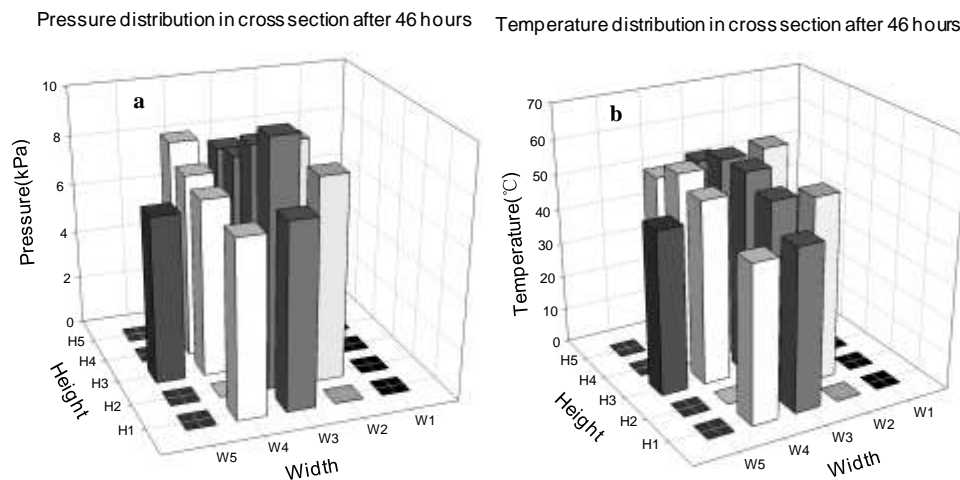


Fig. 8. Pressure and temperature distribution in cross-section after 46 h: (a) pressure distribution and (b) temperature distribution

Relationship between Pressure, Temperature, and Moisture Content during RF/V Drying

As explained above, pressure variations in wood cross-section depends on local permeability, distance to ambient conditions, and local moisture content. Figure 9 shows that the pressure at the four locations decreased quickly (other locations in cross-section can be seen in Fig. 6) until FSP in the curves in the central vertical zones (H direction) after reaching control temperature, and combined with fast MC reduction. During this stage, free water changed to vapor, which was removed through the fiber direction and transverse direction by the driving force of pressure difference; the moisture content therefore dropped quickly. Below the FSP, even with temperature remaining relatively constant, the pressure decreased slowly combined with slow MC reducing until drying end. During this stage, temperatures in all cross-sections were higher than the saturated

temperature corresponding to the pressure at the same location. There was no free water, so only bound water was removed from the wood and became super-heated vapor, which maintained the pressure in wood. The bound water was difficult to remove from bound sites, which resulted a small pressure difference and slow MC reduction.

Locations shown in Fig. 9 are the typical locations (center, intermediate, and outer) in the cross-sections. In this figure, saturated pressure and saturated temperature corresponding to the detected temperature and pressure at the same locations are also plotted. From this figure, we can analyze the relationship between temperature, pressure, and MC. Temperature cannot exceed the saturated temperature if free water is present in wood. It can be seen that the temperature of L5.3 was the earliest one that exceeded the saturated temperature, where free water was initially lost. From that point, the pressure of L5.3 was maintained only by superheated vapor, where it is apparent that temperature was higher than saturated temperature until the end of drying. Site L3.3 was the second point where temperature exceeded the saturated temperature; therefore free water was lost secondly. Free water of the timber disappeared at almost same time as the free water was lost at L3.3, based on the average MC curve. For L4.3 and L2.3, there were some periods in which the temperature overlapped with saturated temperature; after that, free water disappeared, and the temperature exceeded saturated temperature. Free water at L4.3 disappeared after about 18 h, and same phenomenon occurred at L2.3 after 22 h. During these periods, one can see that pressure and saturated pressure overlapped and pressure was maintained only by saturated vapor pressure. This is evident because the temperature detected was equal to the saturated temperature calculated from the detected pressure. For all locations below the FSP, the pressure was lower than the saturated pressure, while temperature was higher than the saturated temperature. Therefore, below the FSP, the pressure in wood was maintained only by superheated vapor, which was generated from the water bound in the cell walls.

Cai *et al.* (2001) and Cai and Hayashi (2001, 2002) investigated the pressure distribution and moisture transfer based on the assumption that pressure is equal to saturated pressure above the FSP. As is well known, pressure performance is affected by wood permeability. Sugi is a species of soft wood that is mainly composed of longitudinal tracheid, ray, and resin canals. The permeability of Sugi is affected by the number of flow paths per unit area, the ratio of average tracheid length to the equivalent thickness of the pit membrane, and the specific permeability coefficient of pit openings (Zhao and Bao 1998). Therefore, the performance of pressure at measured locations was affected by wood permeability and measuring locations. From the curves in Fig. 9 it is apparent that the pressure was higher or equal to the saturated vapor pressure above the FSP. There were only short periods in which the pressure was equal to the saturated pressure, while in most cases the pressure was higher than the saturated pressure due to the residual air in wood for the effect of permeability. One can conclude that the MC was removed by total pressure difference, which was greater than the saturated pressure calculated from the temperature. The driving force was bigger than that in Cai's investigations (Cai *et al.* 2001, 2003; Cai and Hayashi 2001, 2002). Below the FSP, pressure was maintained only by the superheated vapor pressure, which was lower than the saturated pressure, and the MC below the FSP was determined by the relationship between temperature and pressure (Cai and Hayashi 2007; Liu *et al.* 2010).

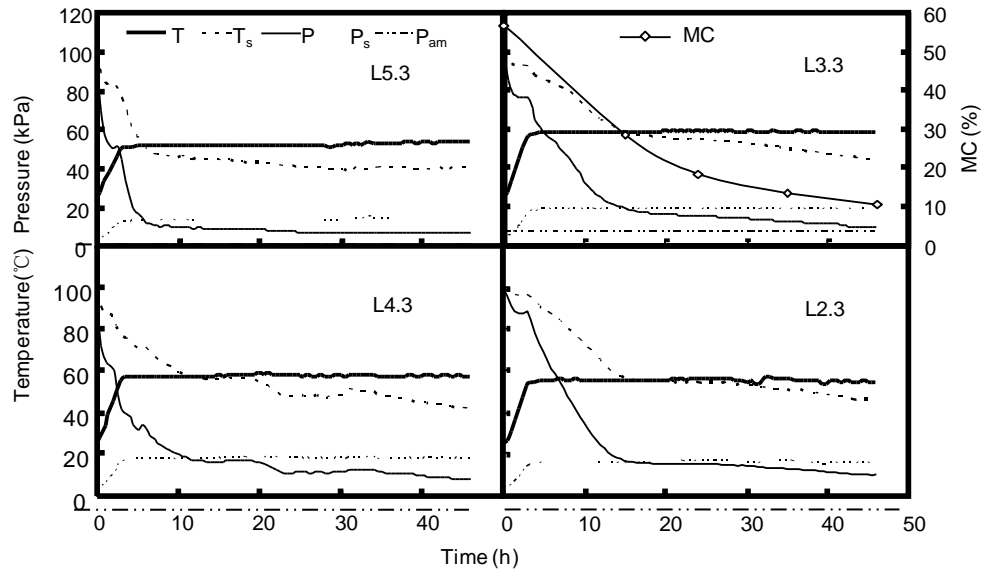


Fig. 9. Variation of temperature (T) and pressure (P) at the same location as well as the corresponding saturated temperature (T_s) and saturated pressure (P_s) at locations 2.3, 3.3, 4.3, and 5.3 during the drying process. MC is the average moisture content curve of the timber during drying.

CONCLUSIONS

1. During radio frequency vacuum drying for sugi wood, the temperature distribution in the wood cross-section was not symmetrical along the height direction, with the highest temperature in the central location. The temperature was lower at locations near the ground electrode plate than those at the opposite feeder electrode plate. Pressure behavior during the drying process was quantified in terms of the pressure reduction rate and water vapor generation rate in wood. Pressure presented irregular variation in the early heating stage of the timber, after which the pressure was higher in the central zones than in the intermediate and surface zones.
2. Three stages of pressure variation in wood cross-section were found, with an irregular variation stage and rapid decreasing stage above the fiber saturation point (FSP) and a slow decreasing stage below the FSP. Above the FSP, pressure was greater than or equal to the saturated pressure (P_s) corresponding to the temperature; below the FSP, the pressure was smaller than P_s . Above the FSP, if pressure was greater than the saturated pressure, the pressure in wood was caused not only by water vapor but also by air; otherwise, the pressure was equal to the saturated pressure when the air was removed completely. Below the FSP, the pressure was maintained only by superheated water vapor pressure. The pressure constant period is the key point to judge whether free water is present or not.
3. Pressure difference was the dominating driving force for moisture removal under RF/V drying. Most of the moisture was quickly removed as water bulk flow and vapor bulk flow above the FSP by the greater pressure difference; below the FSP, the

moisture content decreased slowly as vapor moving due to the smaller pressure difference.

ACKNOWLEDGMENTS

This study was financially supported by the second batch of Special University-Industry Cooperation Research Funds of Zhongshan (grant no. 2013C2FC0038), the Special Foundation for Forestry Science and Technology Innovation of Guangdong Province (grant no. 2011KJCX015-01), and the National Natural Science Foundation of China (grant no. 30972306)

REFERENCES CITED

- Anastasios, K., Stavros, A., and Savvas, G. H. (2001). "Radio frequency vacuum drying of wood. II. Experimental model evaluation," *Drying Technology* 19(1), 85-98.
- Avramidis, S., Liu, F., and Neilson, B. J. (1994). "Radio-frequency/vacuum drying of softwoods: Drying of thick western red cedar with constant electrode voltage," *Forest Products Journal* 44(1), 41-47.
- Cai, Y. C., and Hayashi, K. (2001). "Pressure and temperature distribution in wood during RF/vacuum drying," *Proceedings of the 7th International IUFRO Wood Drying Conference*, Tuskuba, Japan, pp. 386-391.
- Cai, Y. C., and Hayashi, K. (2002) "Contribution of evaporation from transverse sections to drying rate during radio-frequency/vacuum drying (in Japanese)," *Mokuzai Gakkaishi*, 48(2), 73-79.
- Cai, Y. C., and Hayashi, K. (2007). "New monitoring concept of moisture content distribution in wood during RF/vacuum drying," *Journal of Wood Science* 53(1), 1-4.
- Cai, Y. C., Hayashi, K., and Liu, Y. X. (2003). "Moisture transfer mechanism in wood during RF/vacuum drying (in Chinese)," *Proceedings of the 9th National Wood Drying Conference*, Harbin, China, pp. 202-211.
- Cai, Y. C., Hayashi, K., and Sugimori, M. (2001). "Three-dimensional measurement of temperature distribution in wood during radio-frequency/vacuum drying (in Japanese)," *Mokuzai Gakkaishi*, 47(5), 389-396.
- Koumoutsakos, A, Avramidis, S. and S. Hatzikiriakos (2003). "Radio frequency vacuum drying. Part III. Two-dimensional model, optimization and validation," *Drying Technology* 21(8), 1399-1410.
- Liu, H. H., Yang, L., Cai, Y. C., Masatoshi, S., and Hayashi, K. (2010). "Effect of EMC and air in wood on the new in-process moisture content monitoring concept under radio-frequency/vacuum (RF/V) drying," *Journal of Wood Science* 56(2),1-4.
- Noack, D. (1965) "Sonderverfahren der Holz Trocknung Holzwirtschaftliches Jahrbuch Nr.15," *Holz Trocknung*, DRW-verlags-gmbh, Stuttgart, pp. 171-201.
- Perre, P., and Mosnier, S. (1995). "Vacuum drying with radiative heating," *Vacuum Drying of Wood 95*, High Tatras, Slovak, pp. 251-260.
- Resnik, J., Sernek, M., and Kamke, F. A. (1997). "High-frequency heating of wood with moisture content gradient," *Wood and Fiber Science* 29(3), 264-271.

- Ressel, J. B. (1994). "State of the art report on vacuum drying of lumber," *Proceedings of the 4th International IUFRO Wood Drying Conference*, Rotorua, New Zealand, pp. 255-262.
- Sasaki, K., Kawabe, J., and Mori, M. (1987). "Vacuum drying of wood with high frequency heating (II), the pressure within lumber during evacuation and drying (in Japanese)," *Bulletin of the Kyushu University Forests* 57(1), 245-265.
- Taniguci, Y., and Nishio, S. (1993a). "High frequency electric power vacuum drying of wood. V. Change of pressure in wood during drying (in Japanese)," *Mokuzai Gakkaishi* 39(3), 357-362.
- Taniguci, Y., and Nishio, S. (1993b). "High frequency electric power vacuum drying of wood. VI. Gas permeability during vacuum drying and drying characteristics of various species (in Japanese)," *Mokuzai Gakkaishi*, 39(3), 277-283.
- Waananen, K. M., and Pkos, M. R. (1989). "Analysis of mass transfer mechanisms during drying of extruded semolina," *Proceedings of the 5th International Congress on Engineering and Food* (2), 569-578.
- Welling, J. (1994). "Superheated steam vacuum drying of timber-range of application and advantages," *Proceedings of the 7th International IUFRO Wood Drying Conference*, Rotorua, pp. 460-461.
- Zhang, L., Avramidis, S., and Hatzikiriakos, S. G. (1997). "Moisture flow characteristics during radio frequency vacuum drying of thick lumber," *Wood Science and Technology* 31(4), 265-277.
- Zhao, Y. K., and Bao, F.C. (1998). "Theoretical analysis on the relationship between softwood longitudinal permeability and its structure," *Scientia Silvae Sinicae* 34(4), 88-95.

Article submitted: January 7, 2014; Peer review completed: March 29, 2014; Revised version received and accepted: April 1, 2014; Published: April 10, 2014.